



A method to estimate the process noise covariance for a certain class of nonlinear systems

L.I. Gliga^{a,b,*}, H. Chafouk^b, D. Popescu^a, C. Lupu^a

^aDepartment of Automatic Control and Systems Engineering, Faculty of Automatic Control and Computer Science, "Politehnica" University, Bucharest 060042, Romania

^bEmbedded Electronic Systems Research Institute, ESIGELEC, UNIROUEN, Normandy University, Saint Etienne du Rouvray 76800, France



ARTICLE INFO

Article history:

Received 27 July 2018

Received in revised form 14 May 2019

Accepted 26 May 2019

Available online 6 June 2019

Keywords:

Extended Kalman filter

Adaptive

Online covariance estimation

Permanent magnet synchronous generator

ABSTRACT

A new method to compute the covariance matrix of the process noise is presented in this paper. This procedure is shown in the context of an Extended Kalman Filter. However, it does not use any of the matrices of the filter and is therefore independent of it. The method uses a constant covariance matrix for the measurement noise and, at each iteration, it re-computes the values of the process noise covariance matrix. The proposed method and two other ones, selected from the literature, are tested to estimate the current generated by a Permanent Magnet Synchronous Generator. All three methods are tested in the context of the Extended Kalman Filter. The obtained results are compared and discussed to highlight the strengths and weaknesses of the proposed approach.

© 2019 Elsevier Ltd. All rights reserved.

1. Introduction

Newer Wind Turbines (WTs) are equipped with Permanent Magnet Synchronous Generators (PMSGs). These PMSGs generate more electrical energy than induction generators and they do not require a gearbox. Multiple faults can affect such a machine [1,2], the most common being inter-turn short circuit, rotor demagnetization and eccentricity. These faults are usually detected and identified through signal processing techniques, by monitoring the vibrations of the generator shaft or of the stator. Nonetheless, dedicated sensors raise the cost of the equipment. Research was conducted on generator fault diagnosis and performance monitoring using currents or voltages [3,4], to eliminate the need for dedicated sensors. However, these electrical signals are affected by the change in wind speed and the results obtained from signal processing methods like the Fast Fourier Transform can be erroneous [5].

A possible solution is to generate residuals between the real currents and the estimated ones [6]. A state estimator can be used to ensure the required redundancy. In [7], the authors recommended the Extended Kalman Filter (EKF) for this task. The EKF is widely used as a nonlinear state estimator in navigation and positioning systems. It uses statistical information about the states and the noises affecting a process, namely their covariance matrices.

The equations for the prediction phase of a discrete-time EKF are [8]:

$$\hat{x}_k = f(\hat{x}_{k-1}^*, u_k), \quad (1)$$

* Corresponding author at: Department of Automatic Control and Systems Engineering, Faculty of Automatic Control and Computer Science, "Politehnica" University, Bucharest 060042, Romania.

E-mail address: lavinus.gliga@ieee.org (L.I. Gliga).

$$\hat{y}_k = h(\hat{x}_k), \quad (2)$$

$$\hat{P}_k = F_k \hat{P}_{k-1}^* F_k^T + Q_k, \quad (3)$$

where (1) and (2) represent the model of the process. The estimated states are $\hat{x} \in \mathbb{R}^{n_x}$, the inputs are $u \in \mathbb{R}^{n_u}$ and the estimated outputs are $\hat{y} \in \mathbb{R}^{n_y}$. The state function is $f : \mathbb{R}^{n_x+n_u} \rightarrow \mathbb{R}^{n_x}$ and the measurement function is $h : \mathbb{R}^{n_x} \rightarrow \mathbb{R}^{n_y}$. In (3), $\hat{P} \in \mathbb{R}^{n_x \times n_x}$ is the estimated covariance matrix of the error between the estimated and the real states, $F \in \mathbb{R}^{n_x \times n_x}$ is the Jacobian of the state function and $Q \in \mathbb{R}^{n_x \times n_x}$ is the covariance matrix of the process noise. The number of states is n_x , the number of inputs is n_u and the number of measurements is n_y .

The equations for the update phase of an EKF are:

$$K_k = \hat{P}_k H_k^T \left(H_k \hat{P}_k H_k^T + R_k \right)^{-1}, \quad (4)$$

$$\hat{x}_k^* = \hat{x}_k + K_k (y_k - \hat{y}_k), \quad (5)$$

$$\hat{P}_k^* = (I - K_k H_k) \hat{P}_k, \quad (6)$$

where $K \in \mathbb{R}^{n_x \times n_y}$ is the Kalman gain, $H \in \mathbb{R}^{n_y \times n_x}$ is the Jacobian of the measurement function and $R \in \mathbb{R}^{n_y \times n_y}$ is the covariance matrix of the measurement noise. The sampling time is k . The symbol “ \wedge ” stands for an estimation, “ \wedge^* ” denotes the corrected estimation and “ T ” is the transpose of a matrix.

The challenge, when using the EKF, is to find out the covariance matrices for the process and for the measurement noises. If the matrices are not properly chosen, the estimated states might not converge to the real ones. The values of these matrices must be close to the real covariances to ensure the consistency of the estimation. The covariance matrix of the measurement noise can be easily found out using the procedure presented in [9]. It is difficult to select a constant matrix for the process noise, since it is very hard, if not impossible, to estimate the process noise. Even if a good constant covariance matrix could be chosen, one which would guarantee the consistency of the estimated states, it would only be suited for certain values of the noise. If the environmental conditions or the degradation of the equipment would change the intrinsic uncertainties of the process, the covariance would change, and the estimation consistency would no longer be ensured.

The proposed solution is to use an iterative method which could be implemented online. The covariance matrix would be automatically adapted to always ensure the consistency of the estimated states. The method is simple to utilize, but its usage is constrained to certain non-linear systems. Its advantages and limitations are discussed in the conclusions.

The related work will be discussed in Section 2. The estimation method will be explained in Section 3. Simulation results and a comparison with two other procedures will be presented in Section 4. The conclusions and the perspectives will close this paper.

2. Related work

In the scientific literature, different methods are presented to estimate the covariance matrix of the noise affecting a process. However, most of them are designed for the linear Kalman Filter (KF), and they are not usable in an EKF. In other cases, their design limits their applicability.

A similar estimation procedure, to the one proposed in this paper, is presented in [10]. That method is explicitly derived for the KF, and it is not applicable for the EKF. Moreover, the authors of [10] use the following equation to compute the estimation error:

$$\hat{c}\hat{o}\nu(\epsilon_{k+1}, \epsilon_{k+1}) = \frac{k}{k+1} \hat{c}\hat{o}\nu(\epsilon_k, \epsilon_k) + \frac{1}{k+1} \epsilon_{k+1} \epsilon_{k+1}^T, \quad (7)$$

where $\epsilon \in \mathbb{R}^{n_y}$ is the error between the real outputs of the process and the estimated outputs of the model and $\hat{c}\hat{o}\nu(\epsilon_k, \epsilon_k) \in \mathbb{R}^{n_y \times n_y}$ is the covariance matrix of the error at the k th time step. In (7) it is assumed that the mean of the noise is zero. The new method presented in this paper also considers non-zero average values for the noise. Therefore it can be used when sensor faults are present, namely bias [11].

The authors of [12] present an iterative procedure to compute the covariance matrices of the process and of the measurement noises. The method is simple to implement, and it is designed for the EKF:

$$F_k = \frac{1}{N} \sum_{j=k-N+1}^k \epsilon_j \epsilon_j^T, \quad (8)$$

$$Q_k = K_k F_k K_k^T, \quad (9)$$

$$R_k = F_k + H_k P_k H_k^T, \quad (10)$$

where K_k is the Kalman gain obtained in the update phase of the EKF. N is chosen arbitrarily, with no suggestion being provided in [12]. Different values were tested, from the set {1, 10, 100, 1000, 10000}, to find the most suitable one. There is no universal value, and it should be changed according to the uncertainty affecting the process.

Another iterative method, shown in [13], can be used to compute the process and the measurement noises covariances. This procedure is similar to an optimization method with a forgetting factor:

$$Q_k = \alpha Q_{k-1} + (1 - \alpha) \left(K_k d_k d_k^T K_k^T \right), \quad (11)$$

$$R_k = \alpha R_{k-1} + (1 - \alpha) \left(\epsilon_k \epsilon_k^T + H_k P_k H_k^T \right), \quad (12)$$

where $\alpha \in [0, 1]$ is the forgetting factor and $d_k = y_k - h(\hat{x}_k)$ is the a priori estimation error. $\epsilon_k = y_k - h(\hat{x}_k^*)$ is the a posteriori estimation error. In the rest of this paper, the phrase “estimation error” refers to the a posteriori estimation error.

In [14], a procedure is presented to compute the covariance of the process noise. It only uses the estimation error and its covariance. However, the authors assume that the diagonal elements of the covariance matrix of the process noise are equal. In practice, there is no guarantee that the noise has the same linear behavior across all measurement channels. Moreover, the amplitude of the noises might be different, thus the resulting variances – the diagonal elements of the covariance matrix, might not be equal. For example, the engine of a car is influenced differently by the quality of the fuel and the ruggedness of the road.

Another method, shown in [15], is used to determine the covariance matrix of the process noise. The authors assume that the covariance matrix is split, by the anti-diagonal, into two halves: each half has equal elements on its first diagonal, but the values are different between the two halves. While this is a generalization from the previous case, it is still a particular one.

An EKF with three stages is presented in [16]. The second and the third stages are used to improve the estimation obtained from the first one. The method used to compute the process noise covariance matrix has no constraints, compared to the previous two approaches. However, it is very complex as there are three EKFs connected in series. The process and measurement noises covariances are estimated in each stage. As it will be shown in Section 4, even one EKF is very accurate, so the increase in complexity is not necessary (at least for a PMSG).

The procedure presented in this paper was compared with the methods presented in [12,13]. The algorithm to estimate the measurement noise covariance is not published in a peer-reviewed scientific paper. The authors decided to test it, together with the proposed method, against the already established ones.

3. The proposed method

The measurement noise covariance matrix can be easily estimated [9]. The measurement noise affects the data through the sensors. Information about this perturbation is available in the sensor datasheet, as the sensor tolerance or precision. This is the standard deviation of the measurements of the sensor. Thus, the covariance matrix can be computed as:

$$R = \begin{bmatrix} \sigma_1^2 & 0 & \dots & 0 \\ 0 & \sigma_2^2 & \dots & 0 \\ \vdots & \vdots & \ddots & \vdots \\ 0 & 0 & \dots & \sigma_n^2 \end{bmatrix},$$

where $\sigma_i, i = \{1, 2, \dots, n_y\}$ is the standard deviation on each measurement channel. This matrix is diagonal because there is a single sensor on each measurement channel. Therefore, the data acquired by each sensor is only affected by the noise which perturbs that channel.

One possible counter argument to the above reasoning might be that R is constant and the noise covariance might change due to sensor faults or degradation of the equipment. Firstly, sensors are routinely calibrated, at intervals specified by the legislation of each country, or by the manufacturer. This calibration frequency is also mentioned in international standards, such as ISO:9001 [17]. Therefore, the tolerance should remain within the limits specified on the datasheet and the covariance matrix should be constant. Secondly, if the sensor is faulty, it should be replaced. A sensor fault can be quickly diagnosed using an EKF [18].

Thus, only the process noise covariance matrix Q remains to be computed. The nonlinear state-space model of the real process is

$$x_k = f(x_{k-1}, u_k) + w_k, \quad (13)$$

$$y_k = h(x_k) + v_k, \quad (14)$$

where $w_k \in \mathbb{R}^{n_x}$ is the noise or uncertainty which affects the process and $v_k \in \mathbb{R}^{n_y}$ is the perturbation of the measurements. These noises are assumed to be independent and normally distributed. The lack of symbols over the variables means that all of them are the real states and outputs of the process.

The estimation error is

$$\epsilon_k = y_k - \hat{y}_k = h(x_k) + v_k - h(\hat{x}_k), \quad (15)$$

which can be re-written as

$$\epsilon_k = h(f(x_{k-1}, u_k) + w_k) + v_k - h(f(\hat{x}_{k-1}^*, u_k)). \quad (16)$$

Assumption 1. $h : R^{n_x} \rightarrow R^{n_y}$ is a linear function defined as $h(x) = Ax + b$, where $A \in R^{n_y \times n_x}$ is an invertible matrix and $b \in R^{n_y}$ is a vector. Since A is invertible, it is a square matrix and $n_y = n_x$. For simplicity, A and b will be considered constant.

This assumption is restrictive. The number of measurements is usually higher than the number of states and the measurement function is generally nonlinear. There are workarounds around these constraints, which will be the focus of future research. The possible solutions are:

- For a linear measurement function with a non-invertible matrix A , the pseudoinverse can replace the inverse of the matrix;
- A non-linear measurement function can be approximated using Taylor Series Expansion (TSE). For simplicity, it can be linearized by considering only the first term of the TSE, namely the Jacobian matrix. The same reasoning was used to design the EKF. If the Jacobian is not invertible, its pseudoinverse can be used. This Jacobian can be either pre-computed or estimated online using quasi-Newton methods.

Eq. (16) becomes

$$\epsilon_k = h(f(x_{k-1}, u_k)) + h(w_k) + v_k - h(f(\hat{x}_{k-1}^*, u_k)). \quad (17)$$

Assumption 2. The estimation error between the real and the estimated states tends to zero, i.e. $\lim_{k \rightarrow \infty} (x_k - \hat{x}_k) = 0$.

This assumption is also restrictive, since it implies that the covariance matrix of the error tends to zero. However, in usual applications, the covariance may tend to a non-zero value or even non-constant values. In the second case, it would oscillate around a certain set of values for its elements, and the amplitude and frequency of these oscillations would depend on the uncertainties affecting the process. Therefore, the system should have a high observability index, for this method to be used.

Eq. (17) can be reduced to

$$\epsilon_k = h(w_k) + v_k. \quad (18)$$

The covariance matrix of the error can be computed as

$$\hat{\text{cov}}(\epsilon_k, \epsilon_k) = \hat{\text{cov}}(h(w_k) + v_k, h(w_k) + v_k), \quad (19)$$

$$\hat{\text{cov}}(\epsilon_k, \epsilon_k) = \hat{\text{cov}}(Aw_k + v_k + b, Aw_k + v_k + b). \quad (20)$$

b is a constant vector, therefore

$$\hat{\text{cov}}(\epsilon_k, \epsilon_k) = \hat{\text{cov}}(Aw_k + v_k, Aw_k + v_k). \quad (21)$$

The previous equation can be re-written using the bilinearity property of the covariance [19]

$$\hat{\text{cov}}(\epsilon_k, \epsilon_k) = \hat{\text{cov}}(Aw_k, Aw_k) + \hat{\text{cov}}(v_k, v_k) + \hat{\text{cov}}(Aw_k, v_k) + \hat{\text{cov}}(v_k, Aw_k). \quad (22)$$

The noises are independent even when one of them is propagated through the linear transformation A . Therefore, the covariance of the estimation error is equal to

$$\hat{\text{cov}}(\epsilon_k, \epsilon_k) = \hat{\text{cov}}(Aw_k, Aw_k) + \hat{\text{cov}}(v_k, v_k). \quad (23)$$

The previous equation can be rewritten as

$$\hat{\text{cov}}(\epsilon_k, \epsilon_k) = A \cdot \hat{\text{cov}}(w_k, w_k) \cdot A^T + \hat{\text{cov}}(v_k, v_k), \quad (24)$$

which can be reformulated using the specific notations of the EKF

$$\hat{\text{cov}}(\epsilon_k, \epsilon_k) = AQ_kA^T + R. \quad (25)$$

The estimation of the process noise covariance matrix is

$$Q_k = A^{-1}(\hat{\text{cov}}(\epsilon_k, \epsilon_k) - R)(A^{-1})^T. \quad (26)$$

The covariance matrix of the estimation error can be computed online using [20]

$$\hat{\text{cov}}(\epsilon_k, \epsilon_k) = \hat{\text{cov}}(\epsilon_{k-1}, \epsilon_{k-1}) - \frac{\hat{\text{cov}}(\epsilon_{k-1}, \epsilon_{k-1}) - (\epsilon_k - \bar{\epsilon}_k)(\epsilon_k - \bar{\epsilon}_k)^T}{k}, \quad (27)$$

where $\bar{\epsilon}_k$ is the mean of the estimation error, computed at sampling time k .

4. Simulation

The proposed method was tested for an EKF, which was used to estimate the current generated by the PMSG of a direct drive wind turbine. In the simulation, the generator is connected through a three-level back-to-back converter to the grid. The process is modelled in Matlab/Simulink, using the Simscape Power Systems toolbox.

The equations of the PMSG are [7]:

$$\hat{I}_d(t) = -\frac{R_s I_d(t)}{L_s} + \frac{n_p \omega_m(t) L_s I_q(t)}{L_s} + \frac{V_d(t)}{L_s} \quad (28)$$

$$\hat{I}_q(t) = -\frac{R_s I_q(t)}{L_s} - \frac{n_p \omega_m(t) L_s I_d(t)}{L_s} - \frac{n_p \omega_m(t) \phi}{L_s} + \frac{V_q(t)}{L_s} \quad (29)$$

where I_d , I_q , V_d and V_q are the currents (in A) and the voltages (in V) in the dq0 rotor frame. R_s and L_s are the stator resistance (in Ω) and inductance (in H) in the dq0 frame. ω_m is the angular velocity of the generator shaft (in rpm), and ϕ is flux linkage between the permanent magnet rotor and the stator (in Wb).

The states of the model are the currents, and the inputs are the voltages and the angular speed. The model is nonlinear due to the product between a state and an input, in each state equation. The equipment was simulated in nominal operation, when no faults are present. The parameters of the generator are presented in Table 1. The values of the parameters can vary, as shown in [21].

To utilize (28) and (29) in the EKF, the authors used the continuous model with a discrete-time integrator, as shown in [7]. This approach is also used by the Simscape/Power Systems toolbox to discretize the model of the generator, when the user selects a discrete-time simulation.

The proposed method was compared with two others from the literature, namely the ones presented in [12,13].

In a real implementation, the noise cannot be directly measured. The quantifiable measure of performance is the error between the generated and the estimated currents.

In the simulation, the wind speed changes from 8 m/s to 12 m/s, and it is disturbed by a noise with a mean of zero and a variance of 0.2. The profile of the wind speed is shown in Fig. 1.

A word of caution when using the SimScape Power Systems library in Simulink. Although the recommended solver is ode23tb, the simulation might return different results on minor modifications done to the code. This problem can be avoided by using a fixed-step solver with a very low time step. For the simulations presented in this paper, the authors utilized the ode1 solver [22] with a time step of 10^{-6} . A continuous-time solver was selected because the PMSG block from the Simscape Power Systems library can be numerically unstable for discrete simulations.

To test the proposed method, the sensor noise covariance matrix was initialized with the values

$$R = \begin{bmatrix} 0.0001 & 0 \\ 0 & 0.0001 \end{bmatrix}$$

Table 1
Simulation parameters.

Name	Symbol	Value	Unit of Measure	Variation
Stator Resistance	R_s	0.4418	Ω	$\pm 10\%$
Stator Inductance	L_s	0.0014	H	$\pm 7\%$
Flux linkage	ϕ	1.0118^{-14}	Wb	$\pm 2.5\%$
Number of Pole Pairs	n_p	6	N/A	N/A

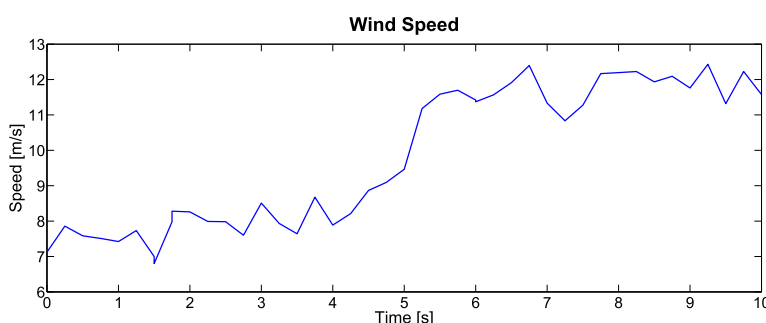


Fig. 1. The profile of the wind speed.

and was kept constant throughout the simulations. These values correspond to a current sensor with a tolerance of 1% [23]. The EKF was implemented to estimate the currents in the dq0 reference frame. However, the estimation error is presented in the abc reference frame.

Initially, no noise was added to the measurements and the parameters of the model were considered constant. The results obtained are shown in Figs. 2–4.

There is a small error around 10^{-14} for all the three methods, due to the way Simscape Power Systems library works: the electrical model is approximated with either a state space model (for continuous or discrete simulations) or with a transfer function model (for phasor simulation) [24].

Due to the limitations of the Simscape Power System toolbox, the parameters of the blocks, which are used to model the electrical components such as the generator, cannot be changed while the simulation is running. Therefore, all possible 27 combinations of parameter values were considered – maximum, minimum and nominal for each one, in the absence of

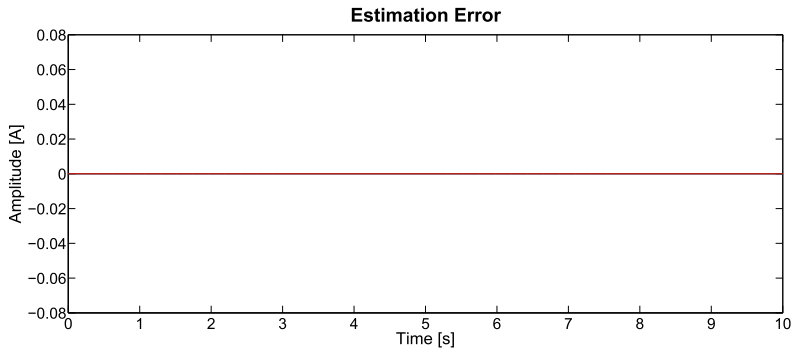


Fig. 2. The error between the generated and the estimated currents using the EKF with the proposed method.

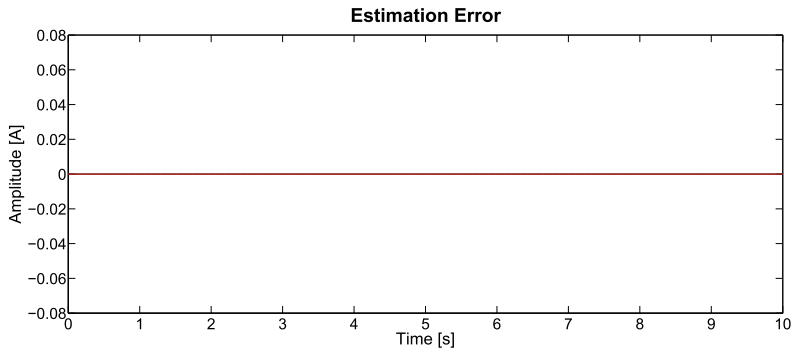


Fig. 3. The error between the generated and the estimated currents using the EKF with the method presented in [12].

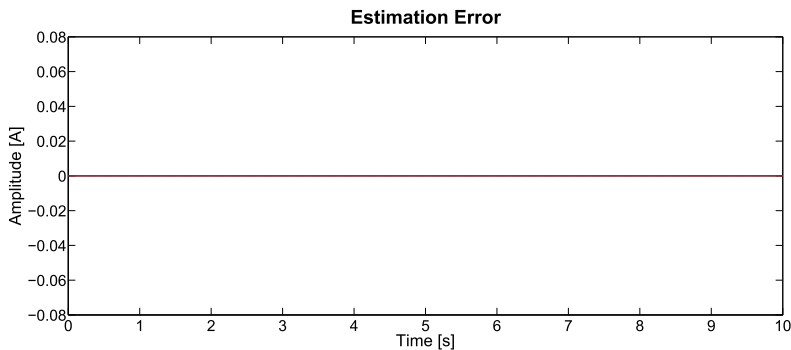


Fig. 4. The error between the generated and the estimated currents using the EKF with the method presented in [13].

perturbations. The results are similar for many combinations. The shown results correspond to a system simulated when R_s is 10% lower, L_s is 7% higher and ϕ is 2.5% lower than their nominal values, and no noise is added.

The results obtained, when the parameters of the process are different than the ones of the model, are shown in Figs. 5, 6, 8. Due to the large estimation error of the method from [12], a zoomed in version is shown in Fig. 7. During a 10 s simulation, the output is continuously increasing, therefore the simulation duration was changed to 30 s, to completely observe the behavior. Because of the very low sampling period, 10^{-6} , the computer would run out of memory for longer simulations.

When the process has different parameters than the model, the EKF which uses the proposed method has the lowest error, less than 0.01 A. It is followed by the EKF which utilizes the procedure from [13]. The method from [12] causes the EKF to become unstable.

Zero-Mean Noises (ZMNs) was added to the signals used by the EKFs. These noises were introduced by the sensors measuring the voltages, the angular velocity of the shaft and the currents. The voltage was perturbed by a noise with a variance of 2, to correspond to a sensor tolerance of 0.5%[25]. The noise affecting the current had a variance of 3.5, as a sensor with a

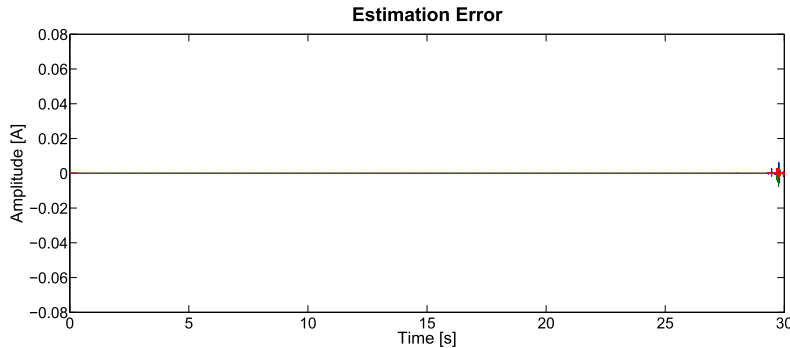


Fig. 5. The error between the generated and the estimated currents using the EKF with the proposed method. The parameters are different than in the nominal case.

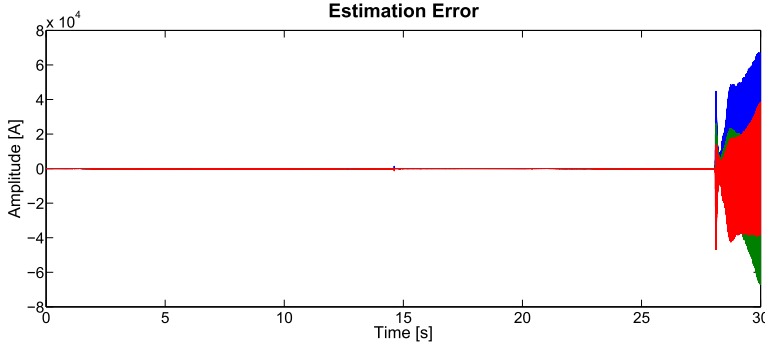


Fig. 6. The error between the generated and the estimated currents using the EKF with the method presented in [12]. The parameters are different than in the nominal case.

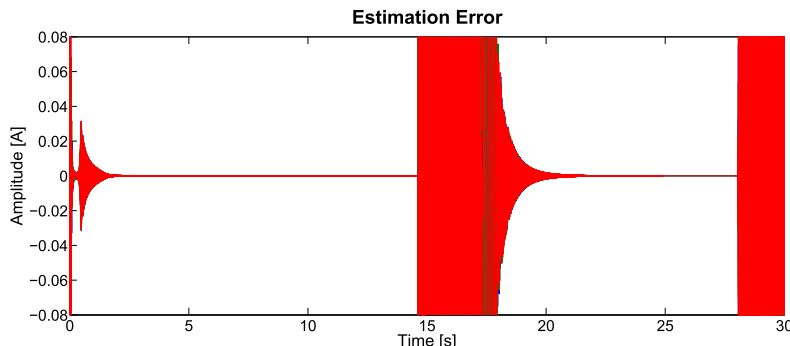


Fig. 7. Zoom in on the estimation error computed using the EKF with the method from [12]. The parameters are different than in the nominal case.

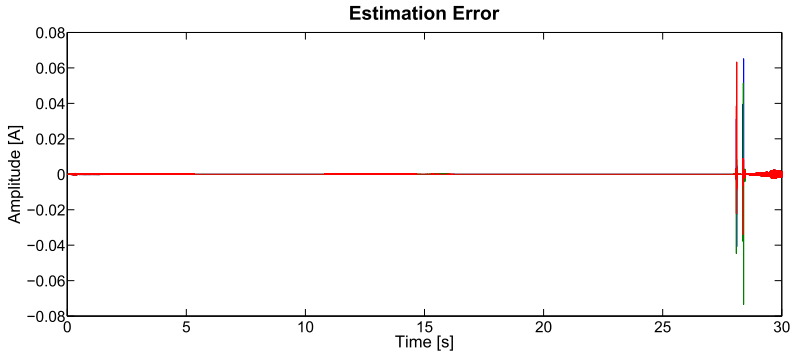


Fig. 8. The error between the generated and the estimated currents using the EKF with the method presented in [13]. The parameters are different than in the nominal case.

tolerance of 1%[23]. The angular velocity was affected by a perturbation with a variance of 14, to simulate a sensor with a tolerance of 1%. The values of the variances were chosen using the assumed tolerance and the maximum amplitudes of these signals. The results are presented in Figs. 9–11.

In Figs. 12–15 are presented the estimation errors in the presence of Non-Zero Mean Noises (NZMN). The noise affecting the voltages has a mean of 1, the one perturbing the angular velocity has a mean of 2 and the current perturbation has a mean of 3. Although these values were chosen arbitrarily, they can represent sensor biases. In this case, there is a DC component in the error. The mean of the error can be used to detect sensor faults. Machine faults can be detected through signal processing techniques applied on the residuals.

The results of all the simulations are summarized in Table 2.

None of the methods seems to be affected by the variation in the wind speed. The only significant difference between them is the speed. The proposed method is the fastest. It is followed by the one from [13] and then the procedure from

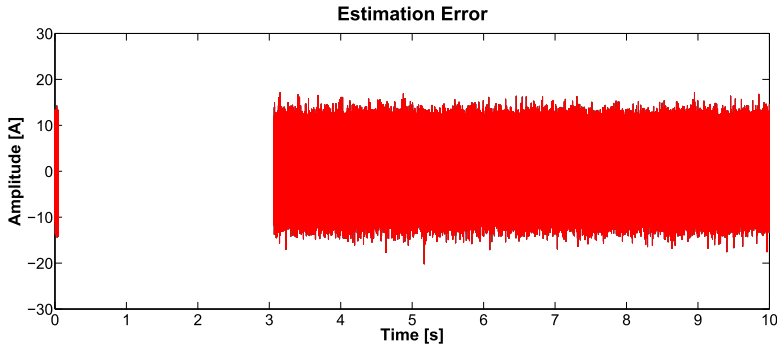


Fig. 9. The error between the generated and the estimated currents using the EKF with the proposed method, in the presence of zero mean noises.

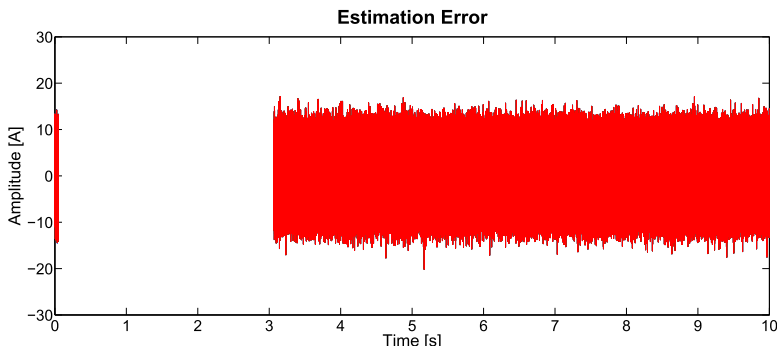


Fig. 10. The error between the generated and the estimated currents using the EKF with the method presented in [12], in the presence of zero mean noises.

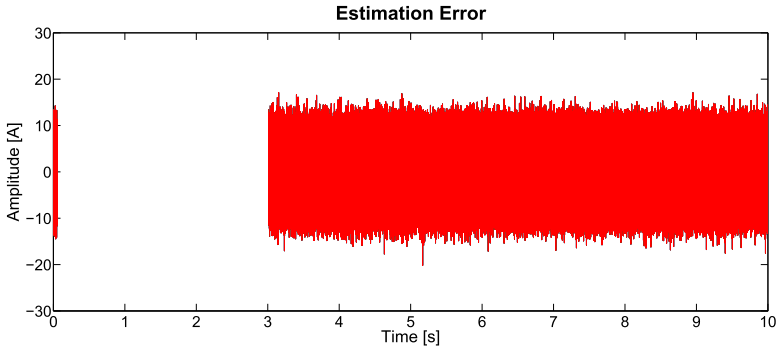


Fig. 11. The error between the generated and the estimated currents using the EKF with the method presented in [13], in the presence of zero mean noises.

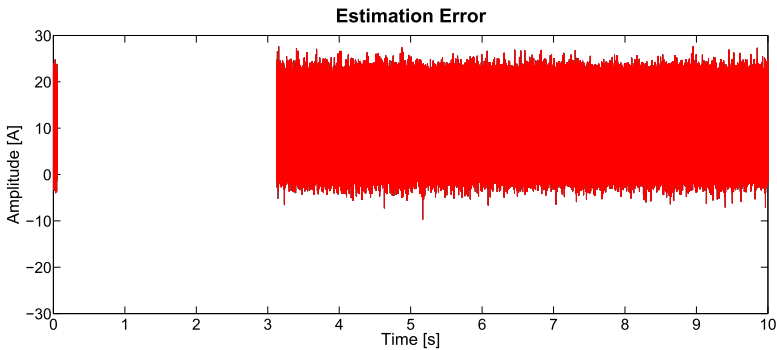


Fig. 12. The error between the generated and the estimated currents using the EKF with the proposed method, in the presence of non-zero mean noises.

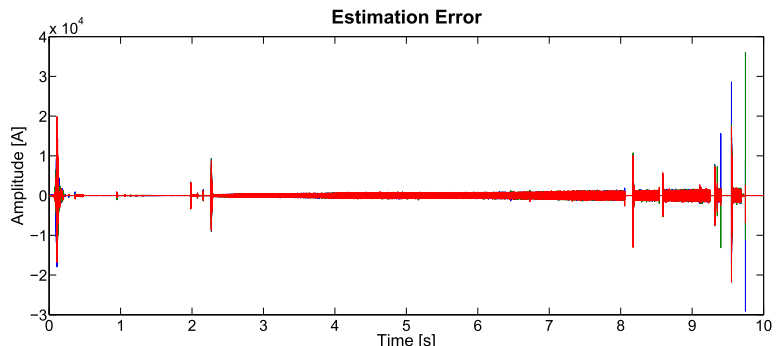


Fig. 13. The error between the generated and the estimated currents using the EKF with the method presented in [12], in the presence of non-zero mean noises.

[12]. The speed of each method was found out by observing the increments of the simulation time, in Simulink. Their values were: 10 for the proposed method, 2 for the one from [12] and 6.66 for the one from [13]. They were later converted to percentage of the speed of the proposed method. These results were obtained using the “Normal” simulation mode in Simulink.

The maximum amplitude of the generated current is around 400 A. In the presence of zero-mean noises, the proposed method has an estimation error of 3.68%, as the one from [13].

The proposed method is very easy to implement, but it requires the covariance matrix of the measurement noise. It is at least as precise as the method from [13], but it is faster, because of the lower complexity. Moreover, it is completely independent of the EKF, and can be used for any algorithm. The potential disadvantage of the proposed method is its reliance on the precomputed covariance matrix of the measurement noise. If this matrix does not closely approximate the real covariance, the estimation of the EKF might not be accurate and precise.

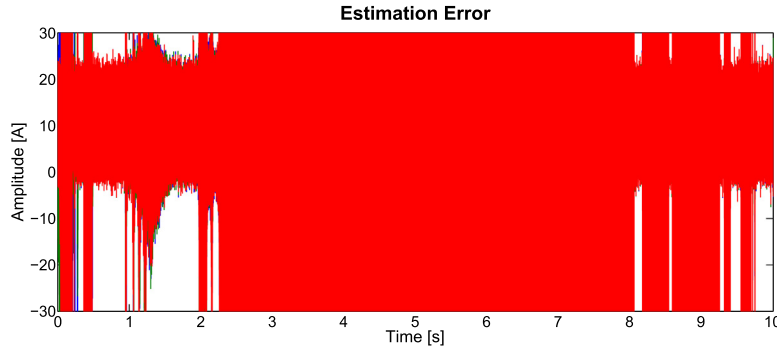


Fig. 14. Zoom in on the error between the generated and the estimated currents using the EKF with the method presented in [12], in the presence of non-zero mean noises.

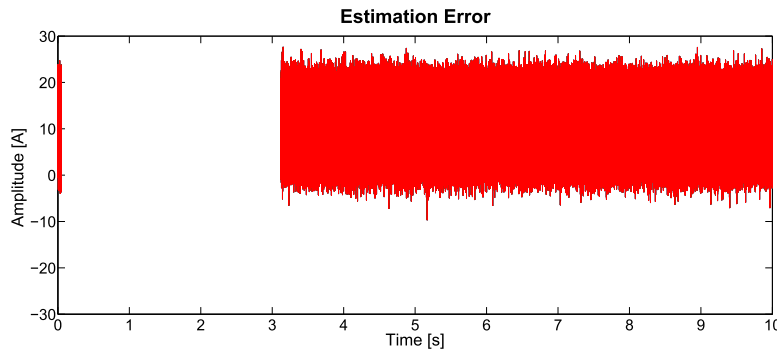


Fig. 15. The error between the generated and the estimated currents using the EKF with the method presented in [13], in the presence of non-zero mean noises.

Table 2
Comparison of the different methods.

Method	RMS Error in presence of				Speed [%]	Applicability
	No noise	ZMNs ^a	NZMNs ^b	DP ^c		
Proposed	$\approx 10^{-14}$	3.5004	11.0669	$\approx 10^{-6}$	100	Any Algorithm
From [12]	$\approx 10^{-14}$	3.5051	347.9036	$\approx 10^{+3}$	20	Only the EKF
From [13]	$\approx 10^{-14}$	3.5004	11.0669	$\approx 10^{-4}$	66.6	Only the EKF

^a Zero Mean Noises.

^b Non-Zero Mean Noises.

^c Different Parameters.

The procedure from [12] is the slowest. Its accuracy and precision are lower than the other two. It can only be applied for the EKF.

The method from [13] can be used only for the EKF. In simulation, the forgetting factor α was chosen equal to 0.5.

The frequency of the errors is mainly due to the very small sampling period used for the simulation, 10^{-6} . In the simulation, noise is generated at each sampling moment, while the parameters of the process retain their nominal values. Due of the lack of a filter, the noise was directly propagated in the current. Moreover, the simulation duration is 10 s, and the frequency of the generated current is 50 Hz. In each figure are shown the three phases currents, therefore 1500 oscillations in total.

The estimations of the noise covariance matrices, in the nominal case, are:

- For the simulations without perturbations:
 - The proposed method:

- * The elements on the main diagonal of Q have negative values in the order of 10^{-4} while the elements on the anti-diagonal have negative values in the order of 10^{-25} .
- The method from [12]:
 - * The elements of Q are zero.
 - * The elements of R have values in the order of 10^{-35} on the diagonal and in the order of 10^{-36} on the anti-diagonal.
- The method from [13]:
 - * The elements on the main diagonal of Q have positive values in the order of 10^{-24} and 10^{-22} , while the elements on the anti-diagonal have positive values in the order of 10^{-23} .
 - * The elements of R have values in the order of 10^{-3} on the diagonal, and a negative element in the order of 10^{-23} together with another positive one in the order of 10^{-24} on the anti-diagonal.
- For the simulations with zero mean noises:
 - The proposed method:
 - * The elements on the main diagonal of Q have positive values in the order of 10^5 while the elements on the anti-diagonal have negative values in the order of 10^5 .
 - The method from [12]:
 - * The elements on the main diagonal of Q have positive values in the order of 10^{11} while the elements on the anti-diagonal have negative values in the order of 10^9 .
 - * The elements of R have values in the order of 10^1 , namely 10.4 and 33.46 on the main diagonal and 18.65 on the anti-diagonal.
 - The method from [13]:
 - * The elements on the main diagonal of Q have positive values in the order of 10^6 while the elements on the anti-diagonal have negative values in the order of 10^6 .
 - * The elements of R have values in the order of 10^{-3} , with negative elements, of the same order, on the anti-diagonal.
- For the simulations with non-zero mean noises:
 - The proposed method:
 - * The elements on the main diagonal of Q have positive values in the order of 10^{10} while the elements on the anti-diagonal have negative values in the order of 10^{10} .
 - The method from [12]:
 - * The elements on the main diagonal of Q have positive values in the order of 10^{11} while the elements on the anti-diagonal have negative values in the order of 10^8 .
 - * The elements of R have the values 0.7655 and 40.26 on the diagonal, respectively 5.552 on the anti-diagonal.
 - The method from [13]:
 - * The elements on the main diagonal of Q have positive values in the order of 10^{11} while the elements on the anti-diagonal have negative values in the order of 10^{11} .
 - * All the elements of R have values in the order of 10^{-1} , with a negative element on the anti-diagonal.
- For the simulation without perturbations, but with different parameters for the process:
 - The proposed method:
 - * The elements on the main diagonal of Q are $\approx 10^{18}$ and $\approx 10^{12}$, while the elements on the anti-diagonal are both $\approx 10^{15}$.
 - The method from [12]:
 - * Both Q and R have values that are not numbers (NaNs in Matlab), hence the instability of the EKF which uses this method.
 - The method from [13]:
 - * The elements on the main diagonal of Q have positive values in the order of 10^{19} and 10^{14} , while the elements on the anti-diagonal have negative values in the order of 10^{17} .
 - * The elements of the first row of R are $\approx -10^7$ and $\approx -10^4$, while the elements on the second row are -1215 and -4735.

The results of the proposed method are very similar to the ones obtained using the procedure presented in [13]. The values of the process noise covariance matrices tend to have similar orders of magnitude. The measurement noise covariance matrix estimated using the method from [13] tends to have lower values than the constant covariance matrix used in the proposed method.

5. Conclusions and perspectives

5.1. Conclusions

A new method, for the estimation of the process noise covariance matrix, was presented in this paper. Although it is shown in the context of an EKF, it is independent of it and can be used with any other type of algorithm. It only uses the measured and estimated signals, and the model of the process.

The procedure only needs an estimation of the covariance matrix of the measurement noise. This can be easily obtained from the datasheets of the sensors, by considering the sensor tolerance as the standard deviation of the data acquired on each channel.

The proposed method was compared with two others, and the simulation results proved its effectiveness. The procedure is simple, fast and precise. The estimation error can be lowered if the measurement signals are filtered before they are input to the EKF. Filters were not used in the simulations.

Moreover, this method can be used for linear systems.

The disadvantages of the proposed method are:

- The measurement function has to be linear, of the form $h(x) = Ax + b$ where the matrix A has to be invertible;
- The number of inputs has to be equal to the number of states;
- The internal states have to be observable.

This procedure can enable the use of the EKF in the fault detection and diagnosis of different equipment. In this paper, a PMSG was simulated, because of the increasing importance of permanent magnet synchronous machines in WTs. The residuals computed using the EKF can be used for sensor and machine fault detection.

5.2. Perspectives

5.2.1. Elimination of the constraints imposed by the assumptions

The first assumption presented in this paper is very restrictive. There are solutions to avoid it, such as using the pseudo-inverse for non-invertible matrices or estimating the Jacobian of nonlinear measurement functions.

The second assumption is also restrictive, as the system must have a high observability index. It should be changed to allow the usage of this method even for less observable systems.

Possible solutions will be the focus of future research.

5.2.2. Sensorless estimation

The inputs of the model presented in (28) and (29) are the angular speed of the rotor shaft and the voltages in the d_q frame. Thus, the only measurements which remain to be used for the state update are the currents. The authors tried to find ways to eliminate the need for current measurement, i.e. to only use the generator speed as an input and the voltages for the state correction. It is possible, but one would have to model the rest of the electrical circuit (back to back converter, transformer, the grid-side filter and the infinite bus). The generator would serve a current source and the voltage drop across the rest of the circuit should be calculated and used to estimate the current in the prediction step of the EKF. The measured voltages would then be used in the update step of the filter. However, such a model might be too computationally heavy to be used in a microcontroller and/or a PLC, i.e. in a real-time implementation. However, a simplified model might be usable.

5.2.3. Covariance estimation

The proposed method requires the covariance matrix of the measurement noise. This necessity can be eliminated by combining the proposed method with the one from [13]. The covariance matrix of the measurement noise could be estimated with the method presented in [13], and the process noise covariance matrix could be estimated as it was proposed in this paper (or vice versa). So, no a priori knowledge of any noise would be necessary. Moreover, the complexity of the method from [13] would decrease, without sacrificing precision. However, the resulting procedure would be tied to the EKF, so it could only be used with it.

5.2.4. Method stability for LTV systems

The inductances and the resistances of the different stator phases can change in case of inter-turn short circuit faults. A study of the resulting system's stability should be conducted to check if the proposed method could be used for systems with time-varying parameters.

Disclosure statement

Declarations of interest: none.

Acknowledgements

The authors thank Bogdan D. Ciubotaru, from “Politehnica” University of Bucharest, for his help in proof-reading this paper and for his useful suggestions on how it may be improved.

This research did not receive any specific grant from funding agencies in the public, commercial, or not-for-profit sectors.

References

- [1] K. Alameh, N. Cit  , G. Hoblos, G. Barakat, Vibration-based fault diagnosis approach for permanent magnet synchronous motors, IFAC-PapersOnLine 48 (21) (2015) 1444–1450, <https://doi.org/10.1016/J.IFACOL.2015.09.728>, URL:<https://www.sciencedirect.com/science/article/pii/S2405896315018571>.
- [2] G. Niu, S. Liu, Demagnetization monitoring and life extending control for permanent magnet-driven traction systems, Mech. Syst. Signal Process. 103 (2018) 264–279, <https://doi.org/10.1016/J.YMSSP.2017.10.003>, URL:<https://www.sciencedirect.com/science/article/pii/S0888327017305290>.
- [3] O.O. Ogidi, P.S. Barendse, M.A. Khan, Fault diagnosis and condition monitoring of axial-flux permanent magnet wind generators, Electric Power Syst. Res. 136 (2016) 1–7, <https://doi.org/10.1016/J.EPSR.2016.01.018>, URL:<https://www.sciencedirect.com/science/article/abs/pii/S0378779616300049>.
- [4] Q. Zhang, L. Tan, G. Xu, Evaluating transient performance of servo mechanisms by analysing stator current of PMSM, Mech. Syst. Signal Process. 101 (2018) 535–548, <https://doi.org/10.1016/J.YMSSP.2017.09.011>, URL:<https://www.sciencedirect.com/science/article/pii/S0888327017304879>.
- [5] J. Faiz, H. Nejadi-Koti, Demagnetization fault indexes in permanent magnet synchronous motors – an overview, IEEE Trans. Magn. 52 (4) (2016) 1–11, <https://doi.org/10.1109/TMAG.2015.2480379>, URL:<http://ieeexplore.ieee.org/document/7273933>.
- [6] L.I. Gliga, H. Chafouk, D. Popescu, C. Lupu, Diagnosis of a permanent magnet synchronous generator using the extended Kalman Filter and the fast Fourier transform, in: 7th International Conference on Systems and Control (ICSC), IEEE, 2018, pp. 65–70, <https://doi.org/10.1109/ICoSC.2018.8587632>, URL:<https://ieeexplore.ieee.org/document/8587632/>.
- [7] L.I. Gliga, H. Chafouk, C. Popescu, Dumitru and comparison of state estimators for a permanent magnet synchronous generator, in: 22nd International Conference on System Theory, Control and Computing (ICSTCC), IEEE, 2018, pp. 474–479, <https://doi.org/10.1109/ICSTCC.2018.8540746>, URL:<https://ieeexplore.ieee.org/document/8540746/>.
- [8] G.H.B. Foo, X. Zhang, D.M. Vilathgamuwa, A sensor fault detection and isolation method in interior permanent-magnet synchronous motor drives based on an extended Kalman filter, IEEE Trans. Indus. Electron. 60 (8) (2013) 3485–3495, <https://doi.org/10.1109/TIE.2013.2244537>, URL:<http://ieeexplore.ieee.org/document/6428675/>.
- [9] S.D. Levy, The extended Kalman filter: an interactive tutorial for non-experts (2016), URL:https://home.wlu.edu/levys/kalman_tutorial/.
- [10] B. Feng, M. Fu, H. Ma, Y. Xia, B. Wang, Kalman filter with recursive covariance estimation-sequentially estimating process noise covariance, IEEE Trans. Indus. Electron. 61 (11) (2014) 6253–6263, <https://doi.org/10.1109/TIE.2014.2301756>, URL:<http://ieeexplore.ieee.org/document/6719478>.
- [11] L.I. Gliga, H. Chafouk, D. Popescu, C. Lupu, Fault Detection and Identification for Fire and Explosion Detection, in: 21st International Conference on Control Systems and Computer Science (CSCS), IEEE, 2017, pp. 43–50, <https://doi.org/10.1109/CSCS.2017.13>, URL:<http://ieeexplore.ieee.org/document/7968541/>.
- [12] Z. Liu, H. He, Sensor fault detection and isolation for a lithium-ion battery pack in electric vehicles using adaptive extended Kalman filter, Appl. Energy 185 (2017) 2033–2044, <https://doi.org/10.1016/J.APENERGY.2015.10.168>, URL:<https://www.sciencedirect.com/science/article/pii/S0306261915014105>.
- [13] S. Akhlaghi, N. Zhou, Z. Huang, Adaptive adjustment of noise covariance in Kalman filter for dynamic state estimation, in: IEEE Power & Energy Society General Meeting, IEEE, 2017, pp. 1–5, <https://doi.org/10.1109/PESGM.2017.8273755>, URL:<http://ieeexplore.ieee.org/document/8273755>.
- [14] Y. Xi, Z. Li, X. Zeng, X. Tang, Q. Liu, H. Xiao, Detection of power quality disturbances using an adaptive process noise covariance Kalman filter, Digital Signal Process. 76 (2018) 34–49, <https://doi.org/10.1016/J.DSP.2018.01.013>, URL:<https://www.sciencedirect.com/science/article/pii/S1051200418300253>.
- [15] Z. Qiu, H. Qian, G. Wang, Adaptive robust cubature Kalman filtering for satellite attitude estimation, Chin. J. Aeronaut. 31 (4) (2018) 806–819, <https://doi.org/10.1016/J.CJA.2018.01.023>, URL:<https://www.sciencedirect.com/science/article/pii/S1000936118300414>.
- [16] M. Xiao, Y. Zhang, Z. Wang, H. Fu, An adaptive three-stage extended Kalman filter for nonlinear discrete-time system in presence of unknown inputs, ISA Trans. 75 (2018) 101–117, <https://doi.org/10.1016/j.isatra.2018.02.007>, URL:<http://www.ncbi.nlm.nih.gov/pubmed/29471968>,<https://linkinghub.elsevier.com/retrieve/pii/S0019057818300661>.
- [17] DNV GL, ISO 9001:2015 Quality Management Systems- Requirements, Tech. rep. (2015). URL:<https://www.dnvgl.be/publications/%0Athe-new-iso-9001-2015-63171..>
- [18] I. Idrissi, R. El bachtiri, H. Chafouk, A bank of Kalman filters for current sensors faults detection and isolation of DFIG for wind turbine, in: International Renewable and Sustainable Energy Conference (IRSEC), IEEE, 2017, pp. 1–6, <https://doi.org/10.1109/IRSection.2017.8477263>, URL:<http://ieeexplore.ieee.org/document/8477263>.
- [19] J. Culic  , D. Ștef  nou, Modelare Analitic   Experimentală Sistemelor, PRINTECH, Bucure  ti, 2008.
- [20] J. Burkholder, Online Covariance (2013). URL:<https://joshuaburkholder.com/wordpress/2013/10/26/%0Aonline-covariance/>.
- [21] S.J. Underwood, I. Husain, Online parameter estimation and adaptive control of permanent-magnet synchronous machines, IEEE Trans. Indus. Electron. 57 (7) (2010) 2435–2443, <https://doi.org/10.1109/TIE.2009.2036029>, URL:<http://ieeexplore.ieee.org/document/5332312/>.
- [22] MathWorks, Choose a Solver (2018). URL: https://fr.mathworks.com/help/simulink/ug/%0Atypes-of-solvers.html?searchHighlight%5C=choose%5C a%5C%0A solver%5C&s_tid%5C=doc%5C_srchtitle.
- [23] LEM, Current Transducer HAIS 50.400-P and HAIS 50.100-TP, Tech. rep. URL:<http://www.farnell.com/datasheets/1681212.pdf>.
- [24] TransEnergie Technologies, SimPowerSystems, Tech. rep. (2003). URL:https://www.mathworks.com/help/releases/R13sp2/pdf_doc/physmod/powersys/powersys.pdf.
- [25] LEM, Voltage transducer DVL 500, Tech. rep. (2013). URL:https://www.lem.com/sites/default/files/products_datasheets/dvl_500.pdf.